Finite-Element Model Updating for Assessment of Progressive Damage in a 3-Story Infilled RC Frame

Babak Moaveni, A.M.ASCE[1]; Andreas Stavridis, A.M.ASCE[2]; Geert Lombaert[3]; Joel P. Conte, M.ASCE[4]; and P. Benson Shing, M.ASCE[5]

Abstract: This paper presents a study on the identification of progressive damage, using an equivalent linear finite-element model updating strategy, in a masonry infilled RC frame that was tested on a shake table. A two-thirds-scale, 3-story, 2-bay, infilled RC frame was tested on the UCSD–NEES shake table to investigate the seismic performance of this type of construction. The shake table tests induced damage in the structure progressively through scaled historical earthquake records of increasing intensity. Between the earthquake tests and at various levels of damage, low-amplitude white-noise base excitations were applied to the infilled RC frame. In this study, the effective modal parameters of the damaged structure have been identified from the white-noise test data with the assumption that it responded in a quasi-linear manner. Modal identification has been performed using a deterministic-stochastic subspace identification method based on the measured input–output data. A sensitivity-based finite-element model updating strategy has been employed to detect, locate, and quantify damage (as a loss of effective local stiffness) based on the changes in the identified effective modal parameters. The results indicate that the method can reliably identify the location and severity of damage observed in the tests. **DOI: 10.1061/(ASCE)ST.1943-541X.0000586.**

CE Database subject headings: Structural health monitoring; Shake table tests; Damage; Finite element method; Frames.

Author keywords: Structural health monitoring; Shake table tests; System identification; Damage identification; Finite-element model updating; Infilled RC frames.

Introduction

A large portfolio of civil structures were designed according to older code provisions that do not meet current safety standards. They may also suffer from aging and deterioration induced by environmental factors, such as corrosive agents and earthquakes. The development of analytical tools to assess the current condition of these structures and to simulate their behavior under different loading scenarios is a task of utmost importance for the engineering community. Such tools can be used to evaluate the present damage incurred by structures and their ability to safely carry future service loads as well as loads from extreme events, such as strong earthquakes. For the simulation of structural performance under different loading conditions, a variety of sophisticated modeling techniques [e.g., see Stavridis and Shing 2010; Koutromanos et al. 2011; for masonry-infilled RC frames] have been developed within the framework of the finite-element (FE) method. A methodology developed to assess the current state of existing structures is vibration-based structural health monitoring, which has attracted increasing attention in the civil engineering research community in recent years and is of growing importance.

Vibration-based, nondestructive damage identification uses changes in the dynamic characteristics of the structure to identify damage. Numerous methods to achieve this goal have been proposed in the literature. Extensive reviews on vibration-based damage identification have been provided by Doebling et al. (1996, 1998) and Sohn et al. (2003). Among these methods is the sensitivity-based FE model updating method (Friswell and Mottershead 1995). In this method, the physical parameters of a FE model of the structure are updated to match the measured modal properties of the structure as damage evolves, and the updated modeling parameters are used to detect, locate, and quantify damage. The determination of the modeling parameters is achieved by minimization of an objective function that measures the discrepancy between the experimentally identified dynamic (modal) properties and those predicted by the FE model. Optimal solutions of the problem are reached through sensitivity-based constrained optimization algorithms.

This concept has been successfully implemented in numerical studies and demonstrated with small-scale physical structural models. However, only a limited number of case studies demonstrate the viability of vibration-based damage identification methods for complex, large-scale structures with realistic design details and damage scenarios. Full- or large-scale dynamic tests of structural specimens provide unique opportunities to evaluate and validate these methods, under realistic conditions, i.e., with the same level of measurement noise, estimation uncertainty, and modeling errors that are observed as in situ condition. This is usually not the case

[1]Assistant Professor, Dept. of Civil and Environmental Engineering, Tufts Univ., 200 College Ave., Medford, MA 02155 (corresponding author). E-mail: babak.moaveni@tufts.edu

[2]Assistant Professor, Dept. of Civil, Structural and Environmental Engineering, Univ. at Buffalo-The State Univ. of New York, Buffalo, NY 14260; formerly, Dept. of Civil Engineering, Univ. of Texas at Arlington, Box 19308, Arlington, TX 76019. E-mail: astavrid@buffalo.edu

[3]Associate Professor, Dept. of Civil Engineering, K. U. Leuven, 3001 Leuven, Belgium. E-mail: Geert.Lombaert@bwk.kuleuven.be

[4]Professor, Dept. of Structural Engineering, Univ. of California at San Diego, 9500 Gilman Dr., San Diego, CA 92093. E-mail: jpconte@ucsd.edu

[5]Professor, Dept. of Structural Engineering, Univ. of California at San Diego, 9500 Gilman Dr., San Diego, CA 92093. E-mail: pshing@ucsd.edu

Note. This manuscript was submitted on April 11, 2011; approved on February 17, 2012; published online on February 22, 2012. Discussion period open until March 1, 2014; separate discussions must be submitted for individual papers. This paper is part of the ***Journal of Structural Engineering***, Vol. 139, No. 10, October 1, 2013. ©ASCE, ISSN 0733-9445/2013/10-1665–1674/$25.00.

for small-/medium-scale model tests under laboratory conditions. Therefore, even if some system and damage identification methods are successfully applied on small-/medium-scale test data, they still need to be validated at full scale in the laboratory and/or in the field. Furthermore, actual construction practices often cannot be reproduced in small-/medium-scale test specimens. The few instances of successful application of FE model updating methods for the condition assessment of large-scale structures include the damage identification studies on the Z24 Bridge in Switzerland (Teughels and De Roeck 2004), the use of dynamic strain measurements from fiber optic sensors for FE model updating of the Tilff Bridge (Reynders et al. 2007), the use of a neural network method based on modal frequencies and a validated FE model to identify the stiffness reduction in a one-third-scaled one-story concrete frame (Zhou et al. 2007), and FE model updating based on identified modal properties of a full-scale composite beam (Moaveni et al. 2008) and a full-scale seven-story RC shear wall building slice (Moaveni et al. 2010).

This paper presents a vibration-based damage assessment study conducted on a 3-story, 2-bay, RC frame with unreinforced masonry infill walls that was tested on the large outdoor shake table at the University of California, San Diego (UCSD). The test frame consisted of a two-thirds-scale subassemblage of a prototype structure designed to have reinforcing details that are representative of the 1920s RC construction in California (Stavridis 2009). This structural specimen was subjected to a series of earthquake base excitations on the shake table. The objective of the tests was to acquire a better understanding of the seismic performance and failure mechanisms of older infilled RC frames that are in existence today. Experimental studies to address this issue have been conducted by other researchers (e.g., Al-Chaar 2002; Hashemi and Mosalam 2006). A more extensive review of research on this topic can be found in Stavridis and Shing (2010). The specimen considered in this study is the largest infilled RC frame dynamically tested on a shake table. The loading sequence was designed to induce damage in the specimen progressively through scaled historical earthquake ground motions of increasing intensity. Between the seismic tests, the infilled frame was subjected to low-amplitude white-noise base excitation. The specimen responded to the white-noise base excitations as a quasi-linear system with modal properties changing as a result of damage. The deterministic-stochastic subspace identification method (Van Overschee and de Moore 1996), based on system input and output signals, has been used to estimate the modal parameters (natural frequencies, damping ratios, and mode shapes) of the structure at the initial undamaged state and at various damage states. The identified modal parameters have then been used in a FE model updating strategy to identify the damage imparted to the structure by the earthquake excitations. The objective function used here for damage identification quantifies the discrepancies between the experimentally identified natural frequencies and mode shapes of the structure and those predicted by the finite-element model of the structure.

This testing program on a masonry infilled RC frame provides a unique opportunity to use dynamic data obtained from a complex large-scale system at various levels of realistically induced damage. Such data cannot be reproduced by numerical simulation, where damage is highly idealized in the form of section reductions of structural members and/or sudden changes in boundary conditions. Nonlinear mechanics-based FE models of such structures able to capture their failure mechanisms are still the subject of active research (Stavridis 2009; Stavridis and Shing 2010). Furthermore, this type of structure presents a challenging problem as the seismic performance of an infilled RC frame depends on the frame–infill interaction and often results in different levels of damage in the infill walls and the bounding frame. Therefore, this structural configuration provides a unique opportunity to evaluate the ability of the considered damage identification method to distinguish and quantify the respective damage in the RC members and masonry walls. At each damage level considered, the damage identification results are compared with the damage observed visually in the specimen or inferred by examination of the various internal and external sensor data collected from the specimen. Successful application of health monitoring methodologies to real structures can provide the owners with a rational tool for decision making regarding the maintenance, evaluation, rehabilitation, and strengthening of the infrastructure especially after natural disasters such as earthquakes.

Shake Table Tests

3-Story Infilled RC Frame

The infilled frame considered here is a two-thirds-scale model of an exterior frame of a prototype structure, designed by Stavridis (2009) to have nonductile reinforcing details representative of the 1920s RC construction in California. The plan view of the prototype structure and the elevation view of the exterior frame are presented in Fig. 1. The design was based on the allowable stress design approach, considering only gravity loads in accordance with engineering practice of that era. However, the design was based on properties of contemporary construction materials, which were used for the construction of this specimen. The frame is infilled with three-wythe unreinforced masonry walls on the exterior. Such structural systems can be found in many existing older buildings in the western United States, including pre-1930s buildings in California. This type of construction is also common in many regions of the world with high seismicity, such as the Mediterranean and Latin America regions.

The specimen tested on the large outdoor shake table at UCSD is shown in Fig. 2. The structure included slabs that simulated the scaled gravity mass of the external frame of the prototype accounting for the two-thirds-length scale factor. Because the prototype structure has infill walls only in its exterior frames, the exterior frames are significantly stiffer and stronger than the interior frames. Consequently, their tributary seismic mass is significantly larger than the gravity mass as illustrated in Fig. 1(a) for the exterior frame along column line A, which was modeled by the test specimen. The test specimen did not have additional gravity load-carrying systems. Therefore, it was decided that the mass carried by the specimen should accurately represent the gravity mass to induce the same vertical stresses as those experienced by the RC columns and infill walls of the prototype. To account for the effect of the seismic mass not included in the specimen, the input ground acceleration time histories had to be scaled in time and amplitude (Stavridis 2009) to satisfy the similitude requirement for the seismic forces. The resulting scale factors for the basic quantities are summarized in Table 1. It should be pointed out that the ground motion levels referred to in the subsequent sections are always with respect to the full-scale prototype structure. Two steel towers were erected on the shake table on the north and south sides of the test specimen to prevent a potential out-of-plane collapse of the structure during severe shaking. These towers did not interact with the structure during the tests as they were placed with a 2-cm gap from the specimen. Further details on the design and configuration of the specimen and the shake table tests can be found in Stavridis (2009) and Stavridis et al. (2012).

Instrumentation Layout

The specimen and steel towers were extensively instrumented with an array of 265 sensors, including 135 strain gauges, 71 string potentiometers and linear variable differential transformers (LVDTs), and 59 uniaxial accelerometers. The accelerometers were used to measure the accelerations along the x, y, and z directions, with x

J. Struct. Eng., 2013, 139(10): 1665-1674

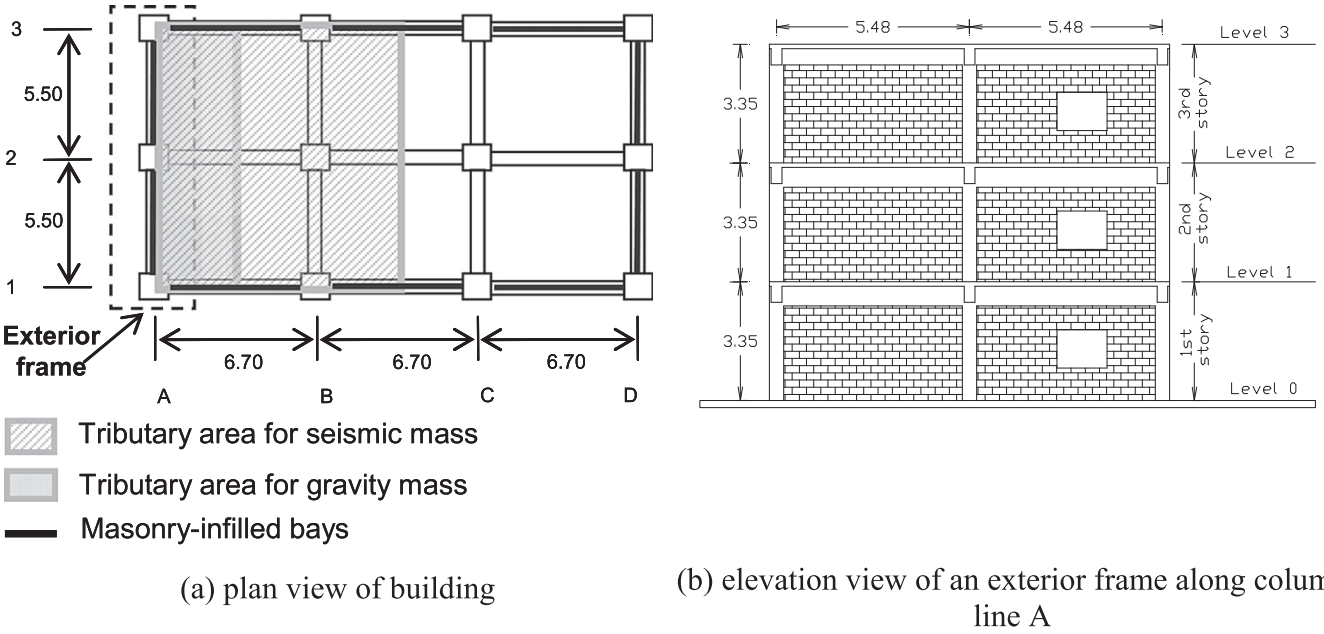

(a) plan view of building

(b) elevation view of an exterior frame along column line A

Fig. 1. Prototype structure (dimensions in meters): (a) plan view of building; (b) elevation view of an exterior frame along column line A

Fig. 2. Front view of the specimen

Table 1. Scale Factors

Quantity	Scaling law	Scale factor
Length	S_L	2/3
Stress	S_σ	1.00
Gravitational acceleration	S_a^g	1.00
Force	$S_F = S_L^2 S_\sigma$	4/9
Gravity mass	$S_m^g = S_F (S_a^g)^{-1}$	4/9
Seismic mass[a]	$S_m^s = S_m^g \lambda_m^{-1}$	0.20
Seismic acceleration	$S_a^s = S_F (S_m^s)^{-1}$	2.27
Time	$S_t = (S_L)^{0.5} (S_a^s)^{-0.5}$	0.54
Frequency	$S_f = S_t^{-1}$	1.85
Strain	S_ε	1.00

[a] $\lambda_m = 2.27$ is the ratio of the seismic mass to the gravity mass carried by the external frame of the prototype

being the direction of the base excitation (longitudinal), y the transverse (out-of-plane) direction, and z the vertical direction. In this study, the measured response from three longitudinal, three vertical, and two transversal acceleration channels on each floor are used (total of 24 channels) to identify the modal parameters of the test structure. The locations of the accelerometers at each floor level are shown in Fig. 3. The measured acceleration responses were sampled at 240 Hz resulting in a Nyquist frequency of 120 Hz, which is significantly higher than the modal frequencies of interest in this study (<60 HZ). Before applying the system identification method to the measured data, all acceleration time histories were band-pass filtered between 0.5 and 70 Hz using a high-order (1024) finite impulse response filter.

Dynamic Tests Performed

The specimen was subjected to a sequence of 44 dynamic tests including ambient-vibration tests, free-vibration tests, and forced-vibration tests (white-noise and seismic base excitations). The main events are shown in Table 2. The testing sequence consisted of earthquake ground motions of increasing intensity. Before and after each earthquake record, low-amplitude white-noise base excitation tests were performed to provide data for the study presented in this paper. The input ground motions were obtained by scaling the time and amplitude of the ground acceleration time history recorded along the NS direction at the Gilroy 3 station during the 1989 Loma Prieta earthquake. For structures with a fundamental frequency close to that of the infilled frame studied here, the Gilroy 3 motion scaled at 67% corresponds to a moderate design level earthquake for Seismic Design Category D, while the original (unscaled) motion corresponds to a maximum considered earthquake (MCE). The MCE event selected as the reference base motion intensity in this study has spectral accelerations, $S_s = 1.5$ g and $S_l = 0.6$ g, and represents the worst-case scenario for San Diego and a moderate scenario for the Los Angeles area (ASCE 2006; Stavridis 2009). In this study, FE model updating for damage identification is performed for seven different damage states of the structure (S0 and S2–S7). Damage state S0 (baseline) corresponds to the uncracked state of the structure before its exposure to the first seismic base excitation, while damage states S1 to S7 correspond to the conditions of the structure after it was subjected to different levels of the Gilroy earthquake. Table 2 summarizes the dynamic tests and the corresponding damage states of the test structure that are considered here.

J. Struct. Eng., 2013, 139(10): 1665-1674

System Identification of the Infilled Frame

The modal parameters of the specimen at each of the considered damage states are identified using the deterministic-stochastic subspace identification (DSI) method (Van Overschee and de Moore 1996), an input–output method, based on data from the low-amplitude (0.03 and 0.04 g RMS) white-noise base excitation tests. Output-only system identification methods, which have been successfully applied for system identification of linear systems (He et al. 2009; Moaveni et al. 2011), are based on the assumption of a broadband (ideal white-noise) input excitation. However, in this set of experiments, the white-noise base excitation inputs were significantly modified by the shake table system dynamics, and consequently, the table motions did not satisfy the broadband assumption as illustrated in Fig. 4 for Test 13. The large outdoor UCSD shake table has an oil column frequency at 10.5 Hz under bare table condition, and the effect of the oil column resonance are mitigated through the use of a notch filter centered at 10.5 Hz in the shake table controller. The large spectral peak just below 10 Hz (Fig. 4) can be attributed to the dynamic interaction between the specimen and the table. More details on the mechanical and dynamic characteristics of the shake table can be found in Ozcelik et al. (2008). The application of output-only system identification methods to these nominal white-noise base excitation test data would result in large estimation errors in the modal parameters, because of deviation of the input excitations from broadband signals.

At each damage state, the DSI method has been applied to 5-min-long filtered input–output data records. The input is the recorded acceleration on the shake table and the output data are the longitudinal, transverse, and vertical acceleration responses of the specimen at various locations. After the records were filtered, an input–output Hankel matrix was formed for each test including 20 block rows with 17 or 18 rows each (one input and 16 or 17 output channels) and 71,962 columns. Fig. 5 shows in polar plots the complex-valued mode shapes of the four most significantly excited modes of the test structure identified at Test 5 (damage state S0). These are the first two longitudinal modes (1-L, 2-L), the second torsional mode (2-T), and the second coupled longitudinal-torsional (2-L-T) mode. The polar plot representation of a mode shape provides information on the degree of nonclassical or nonproportional damping (Veletsos and Ventura 1986) characteristics of that mode. If all components of a mode shape (each component being represented by a vector in a polar plot) are collinear, the vibration mode is classically damped. The more scattered the mode shape components are in the complex plane, the more the structural system is nonclassically damped in that mode. However, measurement noise (low signal-to-noise ratio), estimation errors, and modeling errors can also cause a classically damped vibration mode to be identified as nonclassically damped. From Fig. 5, it is observed that the 1-L, 2-L, and 2-L-T modes at damage state S0 are identified as almost perfectly classically damped, while some degree of nonproportional damping is identified for the 2-T mode.

The real part of the identified mode shapes are shown in Fig. 6. It should be noted that the six measurements perpendicular to the infill wall plane are also used to plot the mode shapes in Figs. 5 and 6. However, Fig. 6 indicates that the longitudinal mode shapes have negligible out-of-plane components. The torsional modes were excited because of imperfections in the construction of the specimen and in the loading conditions, such as an unintended eccentricity between the center of mass and center of stiffness of the specimen, the small yaw rotation of the table induced by table–specimen interaction, and the imperfect geometry and control system of the table. The natural frequencies and damping ratios of the four most significantly excited modes are given in Table 3 for all considered damage states. Modal assurance criterion (MAC) values (Allemang and Brown 1982) were also computed to compare the complex-valued mode shapes identified at each damage state with the corresponding

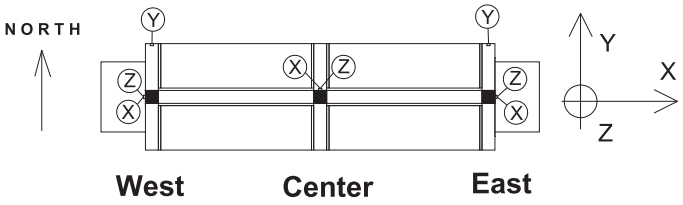

Fig. 3. Locations and directions of accelerometers used in this study on each floor level

Table 2. Dynamic Tests Used in This Study

Test number	Test date	Test description	Damage state
5	11/3/2008	0.03 g RMS WN, 5 min	S0
8	11/3/2008	20% Gilroy EQ	
9	11/3/2008	0.03 g RMS WN, 5 min	S1
12	11/6/2008	40% Gilroy EQ	
13	11/6/2008	0.03 g RMS WN, 5 min	S2
21	11/10/2008	67% Gilroy EQ (DE)	
25	11/12/2008	0.04 g RMS WN, 5 min	S3
26	11/12/2008	67% Gilroy EQ (DE)	
27	11/12/2008	0.04 g RMS WN, 5 min	S4
28	11/12/2008	83% Gilroy EQ	
29	11/12/2008	0.04 g RMS WN, 5 min	S5
33	11/13/2008	91% Gilroy EQ	
34	11/13/2008	0.04 g RMS WN, 5 min	
35	11/13/2008	100% Gilroy EQ (MCE)	
36	11/13/2008	0.04 g RMS WN, 5 min	S6
40	11/18/2008	120% Gilroy EQ	
41	11/18/2008	0.04 g RMS WN, 5 min	S7

Note: WN = white-noise base excitation; EQ = earthquake base excitation; DE = design earthquake; MCE = maximum considered earthquake.

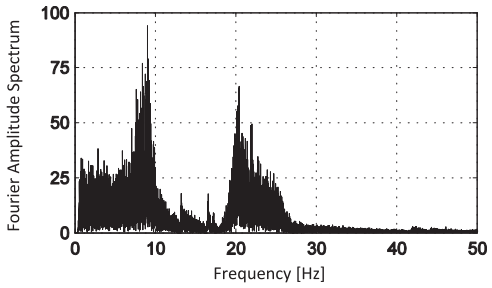

Fig. 4. Fourier amplitude spectrum of the base excitation measured on the shake table during Test 13

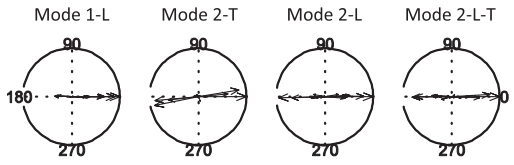

Fig. 5. Polar plot representation of complex mode shapes at damage state S0

J. Struct. Eng., 2013, 139(10): 1665-1674

mode shapes identified at damage state S0. The MAC value, bounded between 0 and 1, measures the degree of correlation between two mode shape vectors ϕ_i and ϕ_j as

$$\mathrm{MAC}(\phi_i, \phi_j) = \frac{|\phi_i^* \phi_j|^2}{|\phi_i|^2 |\phi_j|^2} \quad (1)$$

where * = complex conjugate transpose. The reported modal parameters of the second torsional mode (2-T) are obtained based on longitudinal and transverse acceleration measurements, while the other three modes are identified using longitudinal and vertical acceleration data. This is due to the fact that the transverse components are negligible for the longitudinal mode shapes and relatively small in the 2-L-T mode shape. From Table 3, it is observed that the identified natural frequencies decrease consistently with increasing level of damage, while the identified damping ratios increase. It is noteworthy that the decrease in the natural frequencies of the two longitudinal modes with increasing damage is much more significant than that for the 2-T and 2-L-T modes. A similar observation can be made on the increase of the identified damping ratios. The MAC values, which compare the identified mode shapes at each damage state with their counterpart identified at state S0, also follow a monotonically decreasing trend with increasing damage. The high MAC values (close to one) for damage states S1–S4 indicate that there is little change in the identified mode shapes at these damage states. The identified natural frequencies and mode shapes of the two longitudinal modes are used in the following sections to identify the location and level of damage undergone by the infilled frame in the seismic tests.

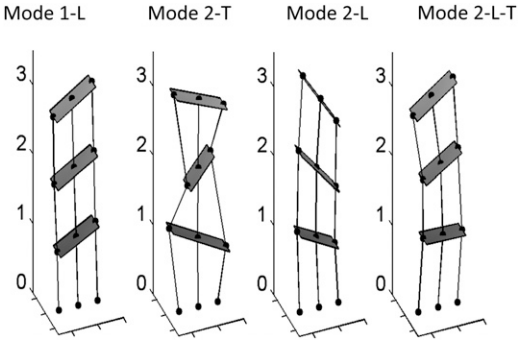

Fig. 6. Vibration mode shapes of the infilled frame at damage state S0

Finite-Element Model Updating for Damage Identification

A sensitivity-based FE model updating strategy (Friswell and Mottershead 1995; Teughels 2003; Teughels and De Roeck 2005) is used to identify damage in the structure at various damage states. The finite-element model of the structure is divided into substructures, in each of which the damage is assumed to be uniformly distributed. In this study, damage is defined as a relative change in the material stiffness (effective modulus of elasticity) of the finite elements in each substructure. Therefore, the effective modulus of elasticity is assumed to be uniform in each substructure (i.e., one effective modulus of elasticity per substructure) and is updated at each considered damage state of the structure through constrained minimization of an objective function.

A linear elastic FE model of the structure is developed using the *MATLAB*-based (MathWorks 2005) structural analysis software FEDEASLab (Filippou and Constantinides 2004). The model consists of 35 nodes interconnected with 54 linear elastic shell and frame elements. Fig. 7 shows the FE model of the structure with the six substructures considered for damage identification. A four-node linear elastic flat shell element with four Gauss integration points available in the literature (Allman 1988; Batoz and Tahar 1982) and implemented in FEDEASLab by He (2008) is used to model the infill walls. The beams and columns of the RC frame are modeled with Bernoulli–Euler frame elements. The distributed mass of the structure is lumped at the nodes of its FE model. The initial FE model of the structure is based on the geometry of the physical specimen and the elastic moduli of the concrete and masonry measured from material tests conducted on the day of the first design level earthquake excitation (67% Gilroy, Test 21) (Stavridis 2009). For the FE model updating, the three columns in each story of the structure are treated as one substructure, and so are the infill walls in the two bays.

Table 3. Modal Parameters of the Infilled Frame Identified at Different Damage States

	Damage state							
Mode	S0	S1	S2	S3	S4	S5	S6	S7
Mode 1-L								
Frequency (Hz)	18.18	18.11	17.99	16.74	15.93	14.78	8.47	5.34
Damping (percentage)	2.0	2.4	1.9	3.3	3.8	6.1	15.7	15.6
MAC	1.00	1.00	1.00	1.00	1.00	0.98	0.80	0.71
Mode 2-T[a]								
Frequency (Hz)	21.16	21.02	21.32	20.77	20.16	19.69	18.20	17.39
Damping (percentage)	1.5	1.5	1.3	1.5	1.8	1.5	1.5	1.6
MAC	1.00	1.00	1.00	0.99	0.98	0.99	0.95	0.68
Mode 2-L								
Frequency (Hz)	41.22	41.09	41.56	40.21	38.56	35.50	27.34	22.57
Damping (percentage)	1.1	1.0	1.0	1.4	3.0	4.4	4.8	4.2
MAC	1.00	1.00	1.00	0.99	0.96	0.92	0.74	0.67
Mode 2-L-T								
Frequency (Hz)	57.81	57.35	57.96	56.25	54.64	52.65	45.98	43.33
Damping (percentage)	1.1	1.3	1.0	0.7	1.2	2.1	2.1	2.7
MAC	1.00	1.00	1.00	0.97	0.92	0.87	0.54	0.29

[a]Mode 2-T is identified based on longitudinal and transverse measurements while the other three modes are identified based on longitudinal and vertical measured data.

J. Struct. Eng., 2013, 139(10): 1665-1674

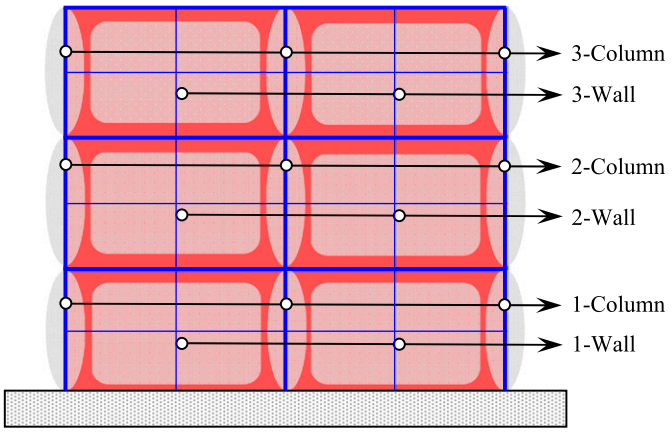

Fig. 7. FE model of the RC frame structure with the six substructures used for damage identification

Hence, the specimen is divided into six substructures. The substructures are selected on the basis of the number and location of the sensors, observability of the updating parameters from the measured data, an effort to limit the total number of updating parameters to avoid ill conditioning, and the authors' experience from previous FE model updating studies (Moaveni et al. 2008, 2010). Moreover, the window openings are ignored, and it is assumed that the solid masonry panel in the west bay and the panel with a window in the east bay have the same modulus of elasticity and exhibit the same level of damage in each story. This is a simplifying assumption that has been made because of the inability of the damage identification procedure to distinguish between damage in the east and west panels due to similar sensitivities of the measured data to the stiffness of the east and west bays of each floor (compensation effects between effective moduli of elasticity in east and west bays). It should be noted that the three longitudinal accelerometers at each floor are attached to the floor slab, which is very stiff in plane, and therefore record very similar acceleration time histories.

The objective function $f(\boldsymbol{\theta})$ used for the identification of the effective material stiffness $\boldsymbol{\theta}$ in each substructure is defined as

$$f(\boldsymbol{\theta}) = \mathbf{r}(\boldsymbol{\theta})^T \mathbf{W}\, \mathbf{r}(\boldsymbol{\theta}) + \left(\mathbf{a}(\boldsymbol{\theta}) - \mathbf{a}^0\right)^T \mathbf{W}^a \left(\mathbf{a}(\boldsymbol{\theta}) - \mathbf{a}^0\right)$$

$$= \sum_j \left[w_j r_j(\boldsymbol{\theta})^2\right] + \sum_k \left[w_k^a (a_k(\boldsymbol{\theta}) - a_k^0)^2\right] \tag{2}$$

where $\boldsymbol{\theta}$ = a set of physical parameters (i.e., the effective moduli of elasticity of the various substructures), which must be adjusted to minimize the objective function; $\mathbf{r}(\boldsymbol{\theta})$ = modal residual vector containing the differences between the experimentally identified and FE predicted modal parameters; $\mathbf{W}$ = diagonal weighting matrix for modal residuals; $\mathbf{a}(\boldsymbol{\theta})$ = vector of dimensionless damage factors representing the level of damage in each of the substructures of the FE model; and $\mathbf{a}^0$ = vector of initial damage factors used as starting point in the optimization process. At each damage state, $\mathbf{a}^0$ is selected as the vector of damage factors identified at the previous damage state, and $\mathbf{a}^0 = \mathbf{0}$ for the first damage state considered (S2) in the model updating procedure. The weighting matrix $\mathbf{W}^a$ for damage factors is a diagonal matrix with each diagonal component representing the relative cost (or penalty) associated with the change of the corresponding damage factor. The weights for damage factors are used for regularization and can reduce the estimation error of the damage factors in the presence of estimation uncertainty in the modal parameters, especially for substructures with parameters to which the employed residuals are less sensitive (Mares et al. 2002). The residual vector $\mathbf{r}(\boldsymbol{\theta})$ in the objective function contains the eigenfrequency, $\mathbf{r}_f(\boldsymbol{\theta})$, and mode shape, $\mathbf{r}_s(\boldsymbol{\theta})$, residuals, which are defined as

$$\mathbf{r}_f(\boldsymbol{\theta}) = \left[\frac{\lambda_j(\boldsymbol{\theta}) - \tilde{\lambda}_j}{\tilde{\lambda}_j}\right]$$

$$\mathbf{r}_s(\boldsymbol{\theta}) = \left[\frac{\phi_j^l(\boldsymbol{\theta})}{\phi_j^r(\boldsymbol{\theta})} - \frac{\tilde{\phi}_j^l}{\tilde{\phi}_j^r}\right] \quad (l \neq r),\ j \in \{1, 2, \ldots, N_m\} \tag{3}$$

where $\lambda_j(\boldsymbol{\theta})$ and $\tilde{\lambda}_j$ = the FE predicted and experimentally identified eigenvalues, respectively, for the jth vibration mode, i.e., $\lambda_j = (2\pi f_j)^2$, in which f_j = corresponding natural frequency; $\boldsymbol{\phi}_j(\boldsymbol{\theta})$ and $\tilde{\boldsymbol{\phi}}_j$ = FE predicted and experimentally identified mode shape vectors, respectively. It should be noted that for each vibration mode, the mode shapes $\boldsymbol{\phi}_j(\boldsymbol{\theta})$ and $\tilde{\boldsymbol{\phi}}_j$ are normalized in a consistent way, i.e., scaled with respect to the same reference component. In Eq. (3), the superscript r indicates the reference component of a mode shape vector, the superscript l refers to the mode shape components that are used in the FE model updating process, which in this case correspond to the degrees of freedom along which the accelerometers measure the acceleration response of the specimen, and N_m denotes the number of vibration modes considered in the damage identification process.

In this study, the natural frequencies and mode shapes of the first two longitudinal vibration modes of the structure are used to form the modal residual vector $\mathbf{r}(\boldsymbol{\theta})$, resulting in a total of 34 residual components, which include two natural frequency residuals and $2 \times (17 - 1) = 32$ mode shape component residuals based on 17 channels of acceleration response measurements. The vector $\mathbf{r}(\boldsymbol{\theta})$ does not include the reference mode shape component used in the normalization. Weights of 1 and 0.5 are assigned to the modal residuals corresponding to the natural frequencies of the first and second longitudinal modes, respectively (i.e., $w_1 = 1$, $w_2 = 0.5$). Weight factors are assigned on the basis of estimation uncertainty of the natural frequency as well as the modal contribution of the corresponding mode. The first vibration mode contributes predominantly to the dynamic response of the structure at all damage states considered, and therefore, its corresponding residuals are assigned a larger weight than the residuals of the second vibration mode. For each mode, the weight factors assigned to mode shape component residuals are equal to the weight factor for the corresponding natural frequency divided by the number of mode shape residuals. The damage factor weights used in the regularization are set to $w_k^a = 0.02 w_1 = 0.02$, with $k = 1, \ldots, n_{\text{sub}}$, where n_{sub} denotes the number of substructures used in the FE model updating process. Finally, the dimensionless damage factors used in the FE model updating process are defined as

$$a_{k,\text{Si}} = \frac{E_k^{S0} - E_k^{\text{Si}}}{E_k^{S0}} \tag{4}$$

where E_k^{Si} = effective modulus of elasticity of substructure k at damage state Si. The preceding damage factors are used in the objective function introduced in Eq. (2).

The optimization algorithm used to minimize the objective function defined in Eq. (2) is a standard Trust Region Newton method (Coleman and Li 1996), which is a sensitivity-based iterative method.

J. Struct. Eng., 2013, 139(10): 1665-1674

The optimization process was performed using the "fmincon" command from the *MATLAB* (MathWorks 2005) optimization toolbox, with the Jacobian matrix and a first-order estimate of the Hessian matrix calculated based on the analytical sensitivities of the modal residuals to the updating parameters. Sensitivities of the eigenfrequencies and mode shapes to the updating parameters are computed using analytical solutions provided by Fox and Kapoor (1968). It is worth mentioning that the use of the analytical Jacobian, instead of the Jacobian estimated through finite difference calculations, increases significantly the efficiency of the computational effort required for minimizing the objective function.

Damage Identification Results

In this study, the FE model updating procedure outlined previously has been implemented to identify and quantify damage in the test structure. The first step in the damage identification process consists of deriving a baseline FE model of the undamaged structure (at state S0), which is used as a reference to quantify damage in the subsequent damage states. In this step, the initial FE model, defined with data available from material tests, is updated to match as closely as possible the identified modal parameters at the undamaged state of the structure by updating the stiffness (effective moduli of elasticity) of the six substructures. This step is performed to account for modeling errors as well as the possible difference between moduli of elasticity of concrete and masonry within each substructure and those obtained from the material tests. The updated model is termed the baseline model to be distinguished from the initial model, which is based entirely on the material test data. The modal properties of the baseline model closely match those identified from the intact structure (see the first row of Table 5).

The effective moduli of elasticity of the different substructures for the initial and the baseline models are summarized in Table 4. The values reported for the initial model correspond to the moduli of elasticity of concrete and masonry infill measured from uniaxial compression tests of concrete cylinders and masonry prisms (Stavridis 2009). Masonry prisms provide the closest representation of a masonry assembly. The prisms used in this study consisted of four stacked brick units connected with mortar joints. From the results reported in Table 4, it is observed that for each substructure, the baseline effective moduli of elasticity differ from the corresponding measured (initial) values. This is due to the fact that the updating parameters (moduli of elasticity) act as effective moduli of elasticity reflecting the overall stiffness of the specimen, accounting for the modeling errors and the contributions of other structural components such as beams for which the stiffness parameters are not calibrated/updated. In this study, a simplifying assumption is made in that the masonry infill is modeled as a homogeneous isotropic material. During the calibration of the initial FE model to obtain the baseline FE model, the "damage factors" defined in Eq. (4) are constrained within the range $[-2, 0.9]$.

Table 4. Effective Moduli of Elasticity of Structural Components in Different Substructures for the Initial and Baseline FE Models

	Effective moduli of elasticity [ksi]	
Substructure	Initial FE model	Baseline FE model (S0)
First-story infills	785	722
Second-story infills	777	901
Third-story infills	946	944
First-story columns	2380	2438
Second-story columns	2530	1935
Third-story columns	2463	2263

Once the baseline model is obtained, the moduli of elasticity of the six substructures (three for infill walls, with one per story, and three for columns, with one per story) shown in Fig. 7 are updated from the baseline FE model (at the undamaged state S0) for damage states S2, S3, S4, S5, S6, and S7. Because of the very small changes in the modal parameters from S0 to S1, FE model updating is not performed at state S1. The stiffness parameters of the elements representing the beams are kept constant at the values used in the baseline FE model. This is a good approximation based on the observed behavior of the physical specimen.

In updating the FE model for each considered damage state of the infilled frame, the dimensionless damage factors are constrained to be in the range $[a^0_{k,\mathrm{Si}}\ 0.99]$ ($k = 1, 2, \ldots, n_{\mathrm{sub}} = 6$). At each damage state, the vector of initial damage factors $\mathbf{a}^0_{\mathrm{Si}}$, used as starting point in the optimization process, is selected as the vector of damage factors identified at the previous damage state. This lower bound is assigned assuming that the damage factors should increase monotonically as the structure was exposed to stronger earthquake base excitations (i.e., damage is irreversible). The damage factors (relative to the baseline FE model) obtained at different damage states are presented in a bar plot in Fig. 8. These results indicate that, as expected, the severity of structural damage increases as the structure was exposed to stronger earthquake excitations, which can be expected because of the accumulation of damage. It is also observed from the results that the extent of the identified damage diminished in the upper stories of the structure with severe damage concentrated in the bottom story, which is indicative of a soft story mechanism. The first measurable damage occurs after the Design Earthquake (DE) at damage state S3, and the largest absolute increase of the damage factor in the bottom story infilled walls (substructure 1-Wall) occurs between damage states S5 and S6 (i.e., during the Maximum Considered Earthquake, MCE).

Table 5 reports the natural frequencies computed from the updated FE model at each considered damage state together with their counterparts identified from white-noise base excitation test data as well as the MAC values between the FE predicted and experimentally identified mode shapes. To compare the mode shapes, only the degrees of freedom corresponding to the locations and orientations of the accelerometers are used for the FE results. From Table 5, it is observed that the FE predicted natural frequencies and mode shapes for the first two longitudinal modes match very well their experimentally identified counterparts. Moreover, the MAC values between the FE predicted and experimentally identified mode shapes are very close to unity for all damage states. The MAC values are in general higher for the first mode than for the second mode.

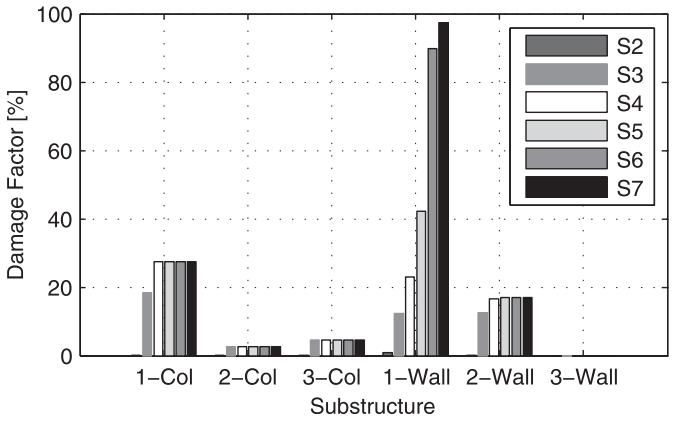

Fig. 8. Identified damage factors in various substructures

J. Struct. Eng., 2013, 139(10): 1665-1674

However, this can be expected because smaller weight factors were assigned to the modal residuals corresponding to the second mode shape.

According to the observations made during the shake table tests, the first noticeable deterioration of the physical specimen occurred during 67% Gilroy, which corresponds to the design earthquake for this structure. After this event, i.e., at damage state S3, the inspection of the physical specimen revealed the first cracks in the structure. Cracks developed along the boundary between the solid infill and the bounding RC frame, and cracks initiated at the window corners for the infill with a window opening. These cracks were insignificant and did not alter significantly either the modal properties or the integrity of the structure. This observation is consistent with the damage identification results in Fig. 8, which show very small damage factors at damage state S2, 18% loss of stiffness in the first story columns, and 12% loss of stiffness in the first story infill walls at damage state S3. Until damage state S5, the stiffness change of the specimen was likely mainly caused by the cracks in the infill walls and at the frame–wall interfaces, which did not jeopardize the strength of the structure.

A significant change in the structural properties is noted at damage state S6, after the specimen was exposed to the 100% Gilroy earthquake record (i.e., MCE). At this stage, dominant cracks were observed in the infills in both bays of the first floor. The cracks already developed in the infills in the previous tests (67, 83, 91% Gilroy) intensified and propagated through all three columns of the first story as shown in Fig. 9. As a result of these major cracks, the specimen fundamental frequency reduced by more than 50%. In the FE model, this translates into a 90% reduction of the stiffness in the first story infills and 28% reduction of the stiffness in the first story columns as indicated in Fig. 8. The 90% reduction of stiffness in the first story infills is larger than what would be expected from visual inspection of the specimen. Therefore, to verify the damage identification results, curves of the total base shear force (scaled up to the prototype structure and normalized with respect to the weight of the specimen) versus first interstory drift ratio are compared in Fig. 10(a) for the white-noise tests performed at damage states S0 (intact structure), S5, S6, and S7. The base shear in this plot is calculated from measured floor accelerations (i.e., inertial base shear) and may exceed the exact base shear because of contribution of damping forces (Goel 2011). From these data, it was estimated that the lateral secant stiffness of the frame was decreased by 53% at S5, 93% at S6, and 97% at S7 as compared with that of the intact structure. It is important to point out that the strength deterioration of the specimen at damage state S6 was considerably less than its stiffness reduction. Indeed, the peak base shear exhibited during the response to 120% Gilroy decreased by only 6% relative to the peak base shear reached during the entire testing sequence (i.e., for 83% Gilroy, Test 26) (Stavridis 2009). During 120% Gilroy (Test 40), additional damage was induced in the specimen. Cracks in the bottom story infills grew significantly (in number, length and width), and a major shear crack developed in the middle column. These cracks further reduced the natural frequency of the first mode to less than one-third of its initial value at state S0. At damage state S7, damage factors of 28% and 97% were identified for the first story columns and infill walls, respectively, while a damage factor of 17% was identified for the second story walls, which developed only minor cracks. This confirms the soft-story mechanism that developed in the structure. The fact that the damage factor of the first story columns remains unchanged at 28% from damage state S4 does not reflect the observed increase of damage in the columns between damages states S4 and S7. This is likely due to the much higher sensitivity of the modal parameters to the stiffness of the infills than to the stiffness of the columns.

In this approach to damage identification, damage is defined as a loss of stiffness in the structure. Therefore, changes in natural periods and mode shapes, which reflect changes in secant stiffness properties of the substructures in the FE model of the specimen, are used in the objective function for damage identification. However, in this particular case, the actual loss of strength of the specimen is found to be significantly less than its stiffness reduction. Furthermore, the identified damage factors are sensitive to the amplitude of the white-noise base excitation to which the structure is assumed to respond quasi-linearly (also found by Moaveni et al. 2010). This can be observed in Fig. 10(b) which compares the response of the specimen in terms of base shear versus first story drift ratio during the first 2.5 s of 100% Gilroy with that from the preceding white-noise test (Test 34). It can be seen that the structure responded inelastically during the white noise test with a secant stiffness matching well that of the initial part of the response to 100% Gilroy.

Table 5. Comparison of FE Computed and Experimentally Identified Modal Parameters

	1-L mode			2-L mode		
Damage state	Exp. Freq	FE Freq	MAC	Exp. Freq	FE Freq	MAC
S0 (baseline)	18.18	17.92	0.99	41.22	42.61	0.96
S2	17.99	17.88	1.00	41.56	42.50	0.95
S3	16.74	16.77	1.00	40.21	40.22	0.98
S4	15.93	15.97	1.00	38.56	38.39	0.99
S5	14.78	14.82	1.00	35.50	35.33	0.99
S6	8.47	8.56	0.99	27.34	24.78	0.99
S7	5.34	5.34	0.99	22.57	22.51	0.97

(a) west column (b) middle column

Fig. 9. Cracks in the infill and columns (west and middle) in the first story at damage state S6 (after 100% Gilroy): (a) west column; (b) middle column

J. Struct. Eng., 2013, 139(10): 1665-1674

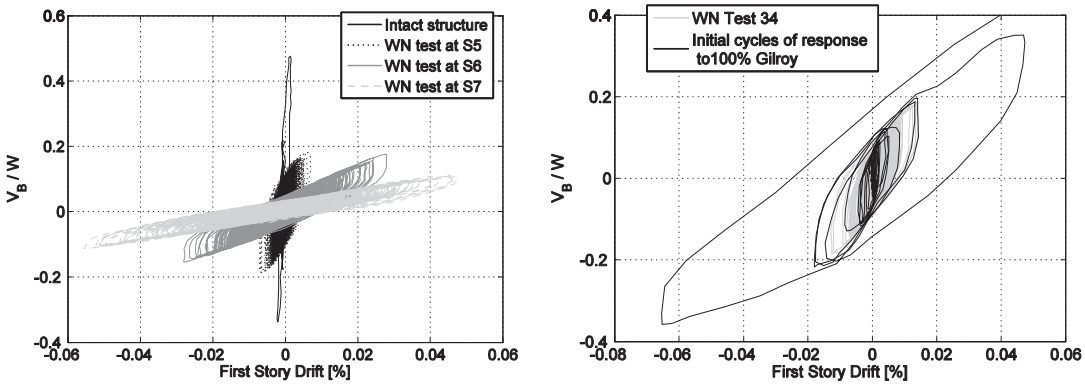

(a) Hysteretic behavior of the structure during white-noise tests at damage states S0 (intact specimen), S5, S6, and S7

(b) Hysteretic behavior of the structure during the initial cycles of response to 100% Gilroy and the preceding white-noise test (Test # 34)

Fig. 10. Base shear versus drift ratio of the first story obtained at different damage states: (a) hysteretic behavior of the structure during white-noise tests at damage states S0 (intact specimen), S5, S6, and S7; (b) hysteretic behavior of the structure during the initial cycles of response to 100% Gilroy and the preceding white-noise test (Test 34)

After this low-amplitude initial response to 100% Gilroy, the structure softened as the amplitude of its displacement increased with increasing intensity of the earthquake excitation.

Conclusions

In this study, a linear FE model updating strategy is applied for vibration-based damage identification of a two-thirds-scale, 3-story, 2-bay, infilled RC frame tested on the UCSD–NEES outdoor shake table. The objective function for damage identification is defined as a combination of natural frequency and mode shape residuals measuring the discrepancy between experimentally identified and FE predicted modal parameters. FE model updating is first used to calibrate the FE model at the undamaged state, which serves as the reference/baseline state, and then applied for damage identification at a number of damage states of the structure. These damage states correspond to states of increasing damage of the physical specimen in the process of being subjected to a sequence of earthquake excitations of increasing intensity.

The damage identification results indicate that the severity of structural damage increases as the structure is exposed to stronger earthquake excitations. The first significant loss of stiffness is identified at damage state S3 (after submission of the design level earthquake), which coincides with the first observation of cracks on the specimen. The largest increase in identified damage factors occurs between damage states S5 and S6, i.e., because of 91 and 100% Gilroy (maximum considered earthquake). This result is consistent with the significant reduction in the secant stiffness of the specimen that was observed from the base shear versus first-story drift hysteresis curves obtained from white-noise tests performed at various damage states including S5 and S6. The damage identification method correctly identifies the spatial distribution of damage in the structure, with the most severe damage at the bottom story and the least damage at the top story. The method also captures the fact that the extent of damage is more significant in the infill walls than in the columns. The analytical modal parameters obtained from the updated FE models are in good agreement with their experimentally identified counterparts, an indication of the accuracy of the updated FE models. However, comparison of the damage identification results and the seismic shake table test results shows that the level of damage identified may not accurately reflect the loss of the structural strength, as loss of stiffness (defined herein as damage) is not well related to actual loss of strength. This motivates the need for new research based on nonlinear FE model updating where calibrated, mechanics-based, nonlinear degrading FE models of structural systems are used to predict both stiffness degradation and strength deterioration.

The following conclusions are drawn from this study and previous work performed by the authors. The damage factors obtained using a linear FE model updating approach are sensitive to the amplitude of the white-noise base excitation to which the structure is assumed to respond quasi-linearly. With increasing level of base excitation and structural damage, the level of nonlinearity in the structural response increases. Therefore, the assumption that the structure behaves as a quasi-linear dynamic system is violated and a linear dynamic model is not strictly able to represent well the behavior of a damaged structure. The spatial distribution (i.e., relative amplitudes) of the identified damage factors, however, is not sensitive to the amplitude of base excitation. Finally, it should be mentioned that the accuracy and spatial resolution of the damage identification results depend significantly on the accuracy and completeness of the identified modal parameters (Moaveni et al. 2009). The estimation variability/uncertainty of the modal parameters can be influenced by several factors, such as the number and types of sensors, measurement noise, length of the data time windows used for system identification, and system identification method used (Moaveni et al. 2013), in addition to the environmental conditions such as the ambient air temperature and relative humidity during data collection (Moser and Moaveni 2011). The variability in the identified modal parameters due to nondamage-related factors needs to be smaller than the changes in these parameters because of damage or compensated for to identify the actual damage in the structure.

Acknowledgments

The shake table tests discussed in this paper were supported by the National Science Foundation Grant No. 0530709 awarded under the George E. Brown, Jr. Network for Earthquake Engineering Simulation (NEES) program. Input from other collaborators at Stanford

J. Struct. Eng., 2013, 139(10): 1665-1674

University and the University of Colorado at Boulder and a Professional Advisory Panel (PAP) during the planning, design, and performance of these shake table tests is gratefully acknowledged. The panel members are David Breiholz, John Kariotis, Gregory Kingsley, Joe Maffei, Ron Mayes, Paul Murray, and Michael Valley. Also, the writers thank the technical staff at the Englekirk Structural Engineering Center of University of California—San Diego and Mr. Ioannis Koutromanos for their assistance in the shake table tests. The opinions expressed in this paper are those of the authors and do not necessarily represent those of the NSF, the collaborators, or the PAP.

References

Al-Chaar, G. (2002). "Evaluating strength and stiffness of unreinforced masonry infill structures." *Rep. No. ERDC/CERL TR-02-1*, U.S. Army Corps of Engineers, Champaign, IL.

Allemang, R. J., and Brown, D. L. (1982). "A correlation coefficient for modal vector analysis." *Proc., 1st International Modal Analysis Conf.*, Society of Experimental Mechanics, Bethel, CT.

Allman, D. J. (1988). "A quadrilateral finite element including vertex rotations for plane elasticity analysis." *Int. J. Numer. Methods Eng.*, 26(3), 717–730.

ASCE (2006). "Minimum design loads for buildings and other structures." *ASCE/SEI 7-05,* Reston, VA.

Batoz, J. L., and Tahar, M. B. (1982). "Evaluation of a new quadrilateral thin plate bending element." *Int. J. Numer. Methods Eng.*, 18(11), 1655–1677.

Coleman, T. F., and Li, Y. (1996). "An interior, trust region approach for nonlinear minimization subject to bounds." *SIAM J. Optim.*, 6(2), 418–445.

Doebling, S. W., Farrar, C. R., and Prime, M. B. (1998). "A summary review of vibration-based damage identification methods." *Shock Vibrat. Digest*, 30(2), 91–105.

Doebling, S. W., Farrar, C. R., Prime, M. B., and Shevitz, D. W. (1996). "Damage identification in structures and mechanical systems based on changes in their vibration characteristics: A detailed literature survey." *Los Alamos National Laboratory Rep. LA-13070-MS*, Los Alamos National Laboratory, Los Alamos, NM.

Filippou, F. C., and Constantinides, M. (2004). "FEDEASLab getting started guide and simulation examples." *Technical Rep., NEESgrid-2004-22*, Univ. of California, Berkeley, CA.

Fox, R. L., and Kapoor, M. P. (1968). "Rates of change of eigenvalues and eigenvectors." *AIAA J.*, 6(12), 2426–2429.

Friswell, M. I., and Mottershead, J. E. (1995). *Finite element model updating in structural dynamics*, Kluwer, Boston.

Goel, R. K. (2011). "Comparison of base shears estimated from floor accelerations and comlumn shears." *Earthq. Spectra*, 27(3), 939–946.

Hashemi, A., and Mosalam, K. M. (2006). "Shake-table experiment on reinforced concrete structure containing masonry infill wall." *Earthquake Eng. Struct. Dynam.*, 35(14), 1827–1852.

He, X. (2008). "Vibration-based damage identification and health monitoring of civil structures." Ph.D. thesis, Dept. of Structural Engineering, Univ. of California, San Diego.

He, X., Moaveni, B., Conte, J. P., Elgamal, A., and Masri, S. F. (2009). "System identification of Alfred Zampa Memorial Bridge using dynamic field test data." *J. Struct. Eng.*, 135(1), 54–66.

Koutromanos, I., Stavridis, A., and Shing, P. B. (2011). "Numerical modeling of masonry-infilled RC frames subjected to seismic loads." *J. Comput. Struct.*, 89(10–11), 1026–1037.

Mares, C., Friswell, M. I., and Mottershead, J. E. (2002). "Model updating using robust estimation." *Mech. Syst. Signal Process.*, 16(1), 169–183.

MathWorks. (2005). *Matlab: High performance numeric computation and visualization software, User's Guide*, MathWorks Inc., Natick, MA.

Moaveni, B., Barbosa, A. R., Conte, J. P., and Hemez, F. M. (2013). "Uncertainty analysis of system identification results obtained for a seven-story building slice tested on the UCSD-NEES shake table." *Struct. Control Health Monit.*, in press.

Moaveni, B., Conte, J. P., and Hemez, F. M. (2009). "Uncertainty and sensitivity analysis of damage identification results obtained using finite element model updating." *J. Comput. Aided Civil Infrastructure Eng.*, 24(5), 320–334.

Moaveni, B., He, X., Conte, J. P., and De Callafon, R. A. (2008). "Damage identification of a composite beam using finite element model updating." *J. Comput. Aided Civil Infrastructure Eng.*, 23(5), 339–359.

Moaveni, B., He, X., Conte, J. P., and Restrepo, J. I. (2010). "Damage identification study of a seven-story full-scale building slice tested on the UCSD-NEES shake table." *Struct. Saf.*, 32(5), 347–356.

Moaveni, B., He, X., Conte, J. P., Restrepo, J. I., and Panagiotou, M. (2011). "System identification study of a seven-story full-scale building slice tested on the UCSD-NEES shake table." *J. Struct. Eng.*, 137(6), 705–717.

Moser, P., and Moaveni, B. (2011). "Environmental effects on the identified natural frequencies of the Dowling Hall Footbridge." *Mech. Syst. Signal Process.*, 25(7), 2336–2357.

Ozcelik, O., Luco, J. E., Conte, J. P., Trombetti, T. L., and Restrepo, J. I. (2008). "Experimental characterization, modeling and identification of the NEES-UCSD shake table mechanical system." *Earthquake Eng. Struct. Dynam.*, 37(2), 243–264.

Reynders, E., De Roeck, G., Bakir, P. G., and Sauvage, C. (2007). "Damage identification on the Tilff bridge by vibration monitoring using optical fibre strain sensors." *J. Eng. Mech.*, 133(2), 185–193.

Sohn, H., Farrar, C. R., Hemez, F. M., Shunk, D. D., Stinemates, D. W., and Nadler, B. R. (2003). "A review of structural health monitoring literature: 1996–2001." *Los Alamos National Laboratory Rep. LA-13976-MS*, Los Alamos National Laboratory, Los Alamos, NM.

Stavridis, A. (2009). "Analytical and experimental seismic performance assessment of masonry-infilled RC frames." Ph.D. dissertation, Dept. of Structural Engineering, Univ. of California, San Diego.

Stavridis, A., and Shing, P. (2010). "Finite-element modeling of nonlinear behavior of masonry- infilled RC frames." *J. Struct. Eng.*, 136(3), 285–296.

Stavridis, A., Koutromanos, I., and Shing, P. B. (2012). "Shake-table tests of a three-story reinforced concrete frame with masonry infill walls." *Earthquake Eng. Struct. Dyn.*, 41(6), 1089–1108.

Teughels, A. (2003). "Inverse modelling of civil engineering structures based on operational modal data." Ph.D. dissertation, Dept. of Civil Engineering, K. U. Leuven, Leuven, Belgium.

Teughels, A., and De Roeck, G. (2004). "Structural damage identification of the highway bridge Z24 by finite element model updating." *J. Sound Vibrat.*, 278(3), 589–610.

Teughels, A., and De Roeck, G. (2005). "Damage detection and parameter identification by finite element model updating." *Arch. Comput. Meth. Eng.*, 12(2), 123–164.

Van Overschee, P., and de Moore, B. (1996). *Subspace identification for linear systems*, Kluwer, Boston.

Veletsos, A. S., and Ventura, C. E. (1986). "Modal analysis of non-classically damped linear systems." *Earthquake Eng. Struct. Dynam.*, 14(2), 217–243.

Zhou, X. T., Ko, J. M., and Ni, Y. Q. (2007). "Experimental study on identification of stiffness change in a concrete frame experiencing damage and retrofit." *Struct. Eng. Mech.*, 25(1), 39–52.